Published in final edited form as:
Chembiochem. 2015 July 06; 16(10): 1502–1511. doi:10.1002/cbic.201500103.

Defining the interaction of human soluble lectin ZG16p and mycobacterial phosphatidylinositol mannosides

Dr. Shinya Hanashima[#[a]], **Dr. Sebastian Götze**[#[b]], **Dr. Yan Liu**[#[c]], **Ms. Akemi Ikeda**[[a]], **Prof. Kyoko Kojima-Aikawa**[[d]], **Prof. Naoyuki Taniguchi**[[e]], **Dr. Daniel Varón Silva**[[b]], **Prof. Ten Feizi**[[c]], **Prof. Peter H. Seeberger**[[b]], and **Dr. Yoshiki Yamaguchi**[*,[a]]

[a]Structural Glycobiology Team, RIKEN-Max Planck Joint Research, Center for Systems Chemical Biology, RIKEN Global Research Cluster, Wako, Saitama 351-0198 (Japan)

[b]Department of Biomolecular Systems, Max Planck Institute of Colloids and Interfaces, Am Mühlenberg 1, 14424 Potsdam (Germany)

[c]Glycosciences Laboratory, Department of Medicine, Imperial College London, W12 0NN (United Kingdom)

[d]The Glycoscience Institute, Ochanomizu University, Otsuka, Bunkyo-ku, Tokyo 112-8610 (Japan)

[e]Disease Glycomics Team, RIKEN-Max Planck Joint Research, Center for Systems Chemical Biology, RIKEN Global Research Cluster, Wako, Saitama 351-0198 (Japan)

[#] These authors contributed equally to this work.

Abstract

ZG16p is a soluble mammalian lectin that interacts with mannose and heparan sulfate. Here we describe detailed analyses of the interactions of human ZG16p with mycobacterial phosphatidylinositol mannosides (PIMs), using glycan microarray and NMR. Pathogen-related glycan microarray analysis identified phosphatidylinositol mono- and di-mannosides (PIM1 and PIM2) as novel ligand candidates of ZG16p. Saturation Transfer Difference (STD) NMR and transferred NOE experiments with chemically synthesized PIM glycans indicate that PIMs preferentially interacts with ZG16p using the mannose residues. Binding site of PIMs is identified by chemical shift perturbation experiments using uniformly ^{15}N-labeled ZG16p. NMR results with docking simulations suggest a binding mode of ZG16p and PIM glycan, which would help to consider the physiological role of ZG16p.

Keywords

phosphatidyl inositol mannoside; NMR; lectin; carbohydrate microarray; chemical synthesis

yyoshiki@riken.jp.

Europe PMC Funders Author Manuscripts

Introduction

ZG16p is a soluble protein that was initially identified in rat pancreas where it is associated with the zymogen granule membrane.[1] The protein was recently detected in the human colon, small intestine, and serum as well as in the pancreas.[2] ZG16p plays a role in packaging pancreatic enzymes into zymogen granules and separating them from constitutively secreted proteins.[3] ZG16p has been considered a primary binding partner of glycosaminoglycans (GAGs) in pancreatic granules.[4]

ZG16p has an amino acid sequence homology with the carbohydrate recognition domain (CRD) of jacalin, a jackfruit lectin.[4–5] A recent X-ray crystallographic analysis revealed that human ZG16p has a jacalin-related β-prism fold, which, in turn, is closely related to Banlec, a mannose-binding lectin in bananas.[5] Previous glycan-microarray screening studies demonstrated that ZG16p has specificity for glycans consisting of mannose, including mannan and Ser/Thr-linked *O*-mannose.[2, 5–6] Asp151 is a key mannose binding residue as evidenced by the mutation of Asp151 to Asn which abolishes glycan binding properties.[2] Interestingly, ZG16p also binds GAGs, especially heparin and heparin sulfate.[4] Our recent crystallographic and NMR studies indicate that the mannose and GAGs binding of ZG16p occurs in distinguishable binding modes.[6] Namely, mannose use a shallow binding site made up of three loops, GG loop (between β1 and β2 strands, Gly31-Gly35), recognition loop (between β7 and β8 strands, Lys102-Tyr104), and binding loop (between β11 and β12 strands, Ser146-Leu149), whereas sulfated oligosaccharides bind to a positively charged surface consisting of a cluster of basic amino acid residues.

Most of the mannose-binding animal C-type lectins, including dendritic cell-specific intercellular adhesion molecule-3-grabbing non-integrin (DC-SIGN), the mannose receptor, Dectin-2, macrophage inducible C-type lectin (Mincle), and Langerin, are involved in host immunity through recognition of mannans of pathogenic bacteria.[7]

The majority of these lectins are signaling molecules which have trans-membrane domains. On the other hand, some of the secreted lectins are also involved in host immunity. Mannose-binding lectin (MBL), a liver-derived serum protein that has a role in the innate immune response by binding to the surface glycans of a wide range of pathogens.[7a, 11] The proteins of the regenerating islet-derived (Reg) family are secreted proteins containing a C-type lectin-like domain, and they play a role in pancreatic function and associated diseases.[12]

Similar to the C-type lectins and Regs, ZG16p binds pathogenic fungi *Candida* and *Malassezia* in a mannose dependent manner.[2] Therefore, it is possible that human ZG16p is involved in the gastrointestinal immune system through binding target glycans of pathogens. In order to get insight into the structure-function relationships of ZG16p for the pathogen recognition, we have determined the glycan-binding specificity of ZG16p using a pathogen-related glycan microarray. ZG16p binds to phosphatidyl inositol mannosides (PIM1 and PIM2, Scheme 1) that are major cell wall components of some pathogenic bacteria including *Mycobacterium tuberculosis*.[16] Further, we have elucidated details of the binding mode of human ZG16p with PIM glycans using NMR and docking simulations.

These findings raise the possibility that human ZG16p may be involved in mucosal defense against bacteria through recognitions of the short PIM glycans.

Results and Discussion

Bacterial infection and host defense mechanisms must be studied from various aspects. The huge diversity of bacterial glycans and the presence of numerous uncharacterized host lectins preclude rapid developments of this research area. The binding preference of human ZG16p lectin is unique in that it involves both mannose and sulfated glycosaminoglycans. However the functional role of ZG16p has not yet been fully characterized in terms of sugar binding. Here we combine glycan array screening, synthetic chemistry and structural biology approaches to elucidate the possible role and mechanism of ZG16p in pathogen recognition.

Pathogen glycan-focused microarray

As we speculated that ZG16p plays a role in the host immune defense by binding cell-wall glycans of pathogenic bacteria, we performed pathogen-related carbohydrate microarray analyses (Figure 1).[17] This array comprised a small set of glycoconjugates, lipid-linked glycans and polysaccharides derived from mycobacteria and fungal pathogens, in addition to mannose-containing neoglycolipids of mammalian type which were tested with ZG16p in another study[6] and served as controls here. The wild type ZG16p gave strong binding signals to PIM1 and PIM2 (arrayed as a mixture), with similar intensities compared to the positive controls including Man-*O*-Thr and Man-*O*-Ser (Figure 1A). Interestingly, the intensity associated with PIM6 was much lower. PIM2 and PIM6 are the two most abundant classes of PIMs found in *Mycobacterium bovis*, *Mycobacterium tuberculosis* H37Rv, and *Mycobacterium smegmatis* 607 (Figure S1).[18] Evidently ZG16p preferentially binds PIM1 and PIM2 rather than PIM6. DC-SIGN through its interaction with PIMs is considered to be a key molecule during infection with *Mycobacterium tuberculosis*.[19] In contrasts to ZG16p, DC-SIGN preferentially binds PIM5 and PIM6, rather than the shorter PIMs.[20] In contrast to the wild type ZG16p, the D151N mutant showed little or no bindings to the abovementioned probes (Figure 1B). This is in accord with a previous report on loss of mannose binding by the mutation.[2] Lipoarabinomannan (LAM) and lipomannan (LM), the major glycolipids found in the cell wall of all the *Mycobacterium* species, elicited little or no binding signals with ZG16p. LAM and LM from *M. tuberculosis*, but not LAM from *M. smegmatis,* which is capped by phosphatidyl inositols, were well bound by plant lectin Concanavalin A (Con A) which was included as a positive control (Figure 1C). No significant binding was observed with ZG16p to *M. tuberculosis* cord factor trehalose-6,6'-dimycolate (TDM), sulfolipids and arabinogalactans, nor to the fungal derived glucan polysaccharides. The glycan array data suggest that ZG16p has a preference for short α-mannose-related glycans, including PIM1 and 2, over the more complex mannose-containing glycans.

Chemical synthesis of PIM1 and PIM2 glycans

To elucidate the binding mode of ZG16p with PIM1 and PIM2 by NMR, we prepared the phosphoglycans **1** and **2** following reported procedures (Scheme 2).[21] Instead of a

phosphodiester bearing a diacylglycerol moiety or functionality that enables covalent attachment to surfaces or beads, PIM1 **1** and PIM2 **2** structures utilized in our experiments required a monoester of phosphoric acid at the C1-position of *myo*-inositol. The syntheses of **1** and **2**, commenced from the common *myo*-inositol building block **3**[22]. To prepare **1**, a temporary PMB ether was selectively placed at the C2 position of **3** followed by benzylation and acidic cleavage to furnish glycosyl acceptor **4** in 58% yield over three steps. Glycosylation of **4** with phosphate **5**[23] at −40 °C in toluene exclusively formed the α-linked pseudodisaccharide **6** in 84% yield (Man-1;$^{1}J_{C1\text{-}H1}$= 175 Hz). Isomerization of the allyl ether using *in situ* generated iridium hydride[24] and hydrolysis of the corresponding enol ether unveiled an alcohol function at the C1 position of the inositol. Phosphonylation with the mixed anhydride of pivalic acid and *H*-phosphonate **7**[25] followed by oxidation provided the triethylammonium salt **8** in 73% yield over three steps starting from **6**. Subjecting **8** to deacetylation and subsequent final hydrogenolysis over palladium in methanol yielded **1** in an excellent yield of 97% over two steps.

The synthesis of **2** continued with a double glycosylation of **3** with glycosylphosphate **5** under conditions similar to those used in synthesis of **6**. Pseudotrisaccharide **9** was obtained in 62% yield and the α-configuration of both anomeric linkages could be confirmed (Man-1;$^{1}J_{C1\text{-}H1}$= 173 and 176 Hz, respectively). Exposure of **9** to $PdCl_2$ in a mixture of CH_2Cl_2 and methanol selectively removed the allyl ether in 64% yield. Final phosphorylation of the corresponding alcohol **10** with phosphonate **7** formed phosphate **11**, which was deacetylated and submitted to hydrogenolysis to provide **2** in 49% yield over four steps.

STD-NMR analysis of the interaction of PIM glycans with ZG16p

To understand the interactions of ZG16p with PIM glycans, Saturation transfer difference (STD)-NMR spectra were recorded (Figure 2). In each case, there is a 100-fold excess of ligand over protein in NMR buffer (PBS, pH 7.4, 99% D_2O). Under the conditions, PIM1 **1** apparently exhibited potent STD-NMR signal, while glycerol indicated as asterisk (*), which could not be fully removed during the purification process of ZG16p, nearly disappeared. The observation clearly indicates that the main constituent of the STD-NMR spectrum shown in Figure 2B reflects the saturation transfer effect from ZG16p. Likewise, PIM2 **2** exhibited potent STD-NMR signals, which confirms their binding to ZG16p (Figure 2C and D).

The relative STD effects (STD%) suggest that the most pronounced interactions between PIMs and ZG16p were via protons at C3 to C6 of the mannose residue (Figure 2E). In the case of the monomannosylated PIM1 **1**, the binding epitope is mainly the pyranose ring at C3-C6 because the protons showed potent saturation effect (70-100%) whereas the inositol moiety received a weaker saturation effect (<70%). Although the data obtained under these conditions must be considered on a rather qualitative basis, this observation is consistent with the crystal structure of ManOMe-ZG16p complex (PDB ID 3VZF), in which C4-C6 of mannose interact with the protein.[6] In the case of PIM2 glycan **2**, protons at M4 and M’4 received similar saturation effect. Although partial signal overlapping at 2, 3 and 5 positions

of two mannoses prevents the precise epitope mapping quantitatively, the data imply that ZG16p interacts with PIM2 using the mannose residues.

TR-NOE analysis of the PIM1 and 2 bound with ZG16p

To investigate the interaction of PIM glycans, we collected ^{1}H-^{1}H NOESY spectra (Figure 3). To minimize the spin diffusion, appropriate mixing time was determined by the NOE build-up curve (Figure S2). 2D ^{1}H-^{1}H NOESY spectrum of PIM1 **1** (4.6-fold excess) in the presence of ZG16p provided a key inter-residual correlation between ManH1-InoH2, and intra-residual correlations in negative NOE sign (Figure 3A). In contrast, the correlation was not observed using the ZG16p-D151N mutant (Figure 3B). The data suggests that the identified NOEs are transferred (TR)-NOEs originating from ZG16p-bound state. The atomic distance of inter-residue ManH1-InoH2 is determined as 2.2 Å from relative volume of the signal.

^{1}H-^{1}H NOESY spectrum of PIM2 **2** (4.6-fold excess) with ZG16p provided inter-residual correlations in ManH1-InoH2, Man'H1-InoH6 and Man'H1-InoH1 in negative NOE sign (Figure 3C). In contrast, only the trace NOE correlations were identified in the control spectrum using ZG16p-D151N (Figure 3D). The atomic distances of the inter-residue protons, ManH1-InoH2, Man'H1-InoH6, and Man'H1-InoH1, are determined to be 2.3, 2.2, and 2.8 Å, respectively. We here apparently observed TR-NOE signals, which also suggests selective binding of PIMs to ZG16p. The binding site was analyzed in following titration experiments.

Chemical shift perturbation experiments of ZG16p with phosphoglycans PIM1 and PIM2

The interaction site/s of the ligands on ZG16p was determined by chemical shift perturbation experiments using ^{1}H-^{15}N heteronuclear single quantum coherence (HSQC) spectra. To achieve this, we prepared uniformly ^{15}N-labeled ZG16p (^{15}N-ZG16p) for ^{1}H-^{15}N HSQC, and ^{13}C,^{15}N-double-labeled ZG16p (^{13}C^{15}N-ZG16p) for sequential signal assignments. The assignment of backbone amide signals of ZG16p was achieved using ^{13}C^{15}N-ZG16p in 2D- and 3D-NMR experiments (Table S1).[29]

PIM1 glycan **1** and PIM2 glycan **2** were titrated into a ^{15}N-ZG16p solution and the signal perturbations were tracked (Figure 4). Results suggested that binding is a fast exchange process because each set of specific signals featured a gradual chemical shift change under the titration conditions.

The results of the titration with PIM1 glycan **1** are depicted in Figure S3 and the weighted ^{1}H/^{15}N chemical shift changes ($\Delta\delta_{avg}$) of ZG16p upon addition of a 20-fold excess of compound **1** is summarized in Figure 5A. The backbone amide signals of Lys36, Arg37, and Gly147 showed large chemical shift changes ($\Delta\delta_{avg} > 0.06$), while those of Gly35, Ser146, and Leu149 were moderate ($0.04 < \Delta\delta_{avg} < 0.06$). Small chemical shift changes ($0.025 < \Delta\delta_{avg} < 0.04$) were observed in Glu29, Tyr30, Gly31, Ser32, Gly33, Gly34, Arg37, Asp82, Asn129, Ile142, Arg145, Asp151, and Ala152. During the titration, Leu149 signal broadened at 20-fold ligand excess. In addition, the signal from Arg37 was strongly affected ($\Delta\delta_{avg}$; 0.06). The K_D of PIM1 **1** was 5.0 mM (Figure S4A).

The backbone amide signals perturbed on titration with PIM2 glycan **2** were very similar to those with PIM1 (Figure 5). The $\Delta\delta_{avg}$ of ^{15}N-ZG16p upon addition of a 20-fold excess of compound **2** (Figure 5B) revealed large chemical shift changes for Gly35, Lys36, Arg37, and Gly147 ($\Delta\delta_{avg} > 0.09$). Moderate chemical shift changes ($0.06 < \Delta\delta_{avg} < 0.09$) were observed for Gly33, Gly34, Ser146, Asp151, and Ala152, and small changes ($0.03 < \Delta\delta_{avg} < 0.06$) for Glu29, Tyr30, Gly31, Ser32, Ile142, Val62, Val76, Asp82, and Arg145. The perturbed signals appeared to broaden at an earlier stage in the titration compared with PIM1 glycan **1**. For example, the signals of Gly35 and Gly147 were broad in the presence of a 20-fold excess of PIM2 glycan **2** while the corresponding signals remain sharp in the presence of a 20-fold excess of PIM1 glycan **1**. Additionally, the Leu149 signal broadened before a 20-fold excess of ligand was reached. These results may reflect that the chemical exchange process induced by PIM2 glycan **2** is similar to the NMR time scale. The titration yielded a K_D for PIM2 glycan **2** of 3.0 mM (Figure S4B). Only limited differences in perturbed backbone NH signals between PIM1 glycan **1** and PIM2 glycan **2**, supports both glycan interacts at the identical binding site.

To clarify the interaction between ZG16p and PIMs, the amino acid residues which show chemical shift perturbations are mapped on the crystal structure (Figure 6).[5] The residues indicated by a heat map color scale are given by the rate of the averaged chemical shift changes in PIM2 titration. The mapping clearly indicates that most of the perturbed residues are localized at the surface of the protein, except for Asp82 and Ile142. The ligand binding site is nearly identical to the mannose specific plant lectins of the family of Jacalin-related lectins having a Greek key motif.[30] They are located in two segments called the GG loop, namely Gly29 to Arg37, and the binding loop, Ser146 to Ala152. The two loops form a shallow ligand-binding site, with Gly33, Gly34, Gly35 and Gly147 below, and Arg37, Arg145, and Lys36 on one side and Asp151 on the other that can accommodate a mannose residue easily.

Model of ZG16p-PIM1 complex

Human ZG16p has a higher affinity for PIM1 glycan **1** and PIM2 glycan **2** (K_D; 5.0 and 3.0 mM, respectively) than the α-methylmannoside (ManOMe, K_D; 15 mM, Figure S4C), even though the contact site epitopes are almost identical. This implies that additional residues, which were not identified by ^{1}H-^{15}N HSQC measurements, may be involved in the phosphoglycan binding. Attempts to co-crystallize ZG16p with either PIM1 **1** or PIM2 **2** were unsuccessful. Therefore a PIM-ZG16p complex model based on the crystal structure of glycerol- ZG16p (PDB ID; 3APA[5]) was constructed. The docking simulation was performed using the software package Glide[31] in Maestro. The resulting models were ranked based on the data obtained by STD and chemical shift perturbation experiments. In this way a feasible model can be distinguished from less likely models. The selected model (Figure 7) was validated by the results from TR-NOE experiments. Atomic distance between H1 of PIM1 Mannose to InoH2 is 2.2 Å from TR-NOE experiments and 2.3 Å in docking simulations.

In the model, interaction of the mannose moiety of PIM1 with ZG16p is mediated through intermolecular hydrogen bonds in backbone of Gly35, Gly147, Ser148 and Leu149, and side

chain of Asp151, originating from GG loop and binding loop (Figure 7). In PIM1, hydroxy groups at 4- and 6-position of mannose are highly involved in the hydrogen bonds. The result is consistent with our chemical shift perturbation experiments and with the binding epitope determined by STD-NMR. The PIM1 mannose binding mode in the model is comparable to the previous X-ray crystal on the complex with ZG16p and ManOMe (Figure S5).[6] However, importantly, the model suggests that another amino acid residue, Tyr104 in recognition loop and side chain of Ser148 in binding loop interact with the inositol moiety. Unfortunately, NMR signals derived from Tyr104 and Ser148 were broadened out in ^{1}H-^{15}N HSQC spectrum possibly due to chemical exchange. Although there is a lack of direct evidence for the interaction of Tyr104 and Ser148, it is very likely that these amino acids support the tighter binding of PIM1 and PIM2 in comparison to ManOMe. In line with this, our structural analysis showed that the hydroxy group of Tyr104 showed water-mediated interaction with Man-*O*-Ser, which assisted ligand binding.[6]

Chemical shift perturbation experiments in PIM2 suggest that the binding mode is similar to PIM1. However, STD-NMR epitope analysis indicates the contribution of two mannoses. One possible explanation is that PIM2 has two independent binding modes using the identical binding site on the protein (Figure S6).

Naturally occurring PIMs have a hydrophobic phosphatidyl group attached at O1-position of inositol, which anchors it to the cell surface of mycobacteria and is crucial for interactions with different human proteins. For example, mouse CD1d, a known receptor of PIMs, has hydrophobic grooves wherein acyl chains of glycolipids are bound.[32] In contrast, ZG16p lacks these structural motifs, and evidently binding of this protein involves the sugar and perhaps the phosphate moiety of PIMs.

Conclusions

We demonstrate that ZG16p preferentially interacts with the *Mycobacterium* glycolipids, PIM 1 and PIM2 and to a lesser extent PIM6 and other mycobacterial glyco-components. STD-NMR studies reveal the interaction of the human lectin with C3-C6 moiety of the mannose residue. NMR signal perturbation experiments demonstrate that the phosphoglycans of PIMs interact with the GG loop (Gly31-Lys36) and the binding loop (Ser146-Asp151) of ZG16p, and that their dissociation constants are three to five-fold lower than those of ManOMe. Docking simulations combined with NMR data implicate Tyr104, located in the recognition loop, in an interaction with the inositol moiety of PIMs. ZG16p may play a role in the mucosal immune response by associating with exogenous short PIMs of pathogenic bacteria, including *Mycobacterium tuberculosis*, and with endogenous glycosaminoglycans using independent binding sites. Further work is certainly required in order to elucidate the physiological function of the lectin.

Experimental Section

Expression and Preparation of ZG16p

Recombinant ZG16p protein, ^{15}N-uniformly labeled ZG16p (^{15}N-ZG16p), and $^{13}C/^{15}N$-uniformly labeled ZG16p ($^{13}C/^{15}N$-ZG16p) were prepared using pCold-MBP (maltose-

binding protein) vector, according to the previously reported procedure with slight modifications.[5] DNA fragments encoding human ZG16p (amino acid residues 21–159; for crystallization, a.a. 21-167; for NMR study, comprising the core lectin domain) were subcloned into pCold-MBP vector[35] for production of recombinant proteins. For microarray analyses, Glutathione-*S*-transferase (GST)-tagged ZG16p protein (21-167) and its mutant GST-ZG16p-D151N were prepared using pCold-GST vector. The plasmid constructs were transformed into *Escherichia coli* BL21(DE3) codon plus (Stratagene) and the cells were grown at 37 °C in either LB, M9 composed with $^{15}NH_4Cl$; (ISOTEC; for ^{15}N-ZG16p), or Spectra 9 (Cambridge Isotope Laboratories, Inc. for $^{13}C/^{15}N$-ZG16p) media. After induction with 0.1 mM isopropyl β-D-thiogalactoside, the cells were cultured at 15 °C for 24 h. Then, the cells were harvested, resuspended and sonicated in a buffer containing 50 mM Tris–HCl (pH 8.0), 50 mM NaCl, and Bugbuster (Novagen). After centrifugation, the supernatants containing $(His)_6$-MBP-fused proteins were collected and applied to a Ni Sepharose column (GE Healthcare) equilibrated with PBS (8 mM Na_2HPO_4, 1 mM KH_2PO_4, 137 mM NaCl, and 3 mM KCl, pH 7.4). After washing with PBS, the proteins were eluted with PBS containing 500 mM imidazole. Then, the $(His)_6$-MBP tag was removed by digestion with Tobacco Etch Virus protease at 4 °C for 12 h. The digested proteins were passed through a Ni-Sepharose column, and final purification was performed with size exclusion chromatography (HiLoad 16/60 Superdex 75 pg; GE Healthcare) or cation exchange chromatography (TOYOPEARL SP-650M or Giga Cap S-650M, TOSOH). The purified proteins were replaced with PBS including 99% or 10% (v/v) D_2O, and final pH were adjusted at 7.4 for ligand observations in STD-NMR and TR-NOESY, and 6.5 for protein observations in ^{1}H-^{15}N HSQC and backbone amide focusing experiments.

Glycan microarray analyses

The microarrays comprised four mannose-containing neoglycolipids (NGLs), nine mycobacterial compounds for antigen preparations received from Biodefense and Emerging Infections Research Resources Repository, and three fungal derived glucan polysaccharides. The list of samples arrayed with their sequences is summarized in Table 1. The arrays were generated robotically using a non-contact arrayer on nitrocellulose coated microarray slides.[17e] All the probes are arrayed with carrier lipids (phosphatidylcholine and cholesterol; both from Sigma) as described,[17e] except for *M. tuberculosis* arabinogalactan and the glucan polysaccharides (positions 17-19) which were arrayed in the absence of the lipid carriers. The lipid-linked probes (positions 1-8) were arrayed at 2 and 5 fmol per spot and these samples were quantified based on primulin staining of lipid tags.[17e] The bacterial and fungal derived glycoconjugates and polysaccharides (positions 9-20) were arrayed at 0.03 and 0.1 ng per spot according to dry weight of the samples received from commercial sources. Microarray analyses with GST-tagged ZG16p proteins GST-ZG16p and GST-ZG16p-D151N mutant were performed as described previously.[17e, 36] In brief, microarray slides were blocked at ambient temperature for 60 min with 3% w/v bovine serum albumin (BSA) in PBS. The GST-ZG16p, GST-ZG16p-D151N and GST were overlaid at 100 μg/mL in the presence of 1% BSA and incubated for 90 min, followed by rabbit anti-GST antibody Z-5 (Santa Cruz), 1:200, and then biotinylated anti-rabbit IgG (Sigma), 1:200. Biotinylated Con A (Vector) was analyzed at 0.5 μg/mL and 15 μg/mL,

respectively. Binding was detected with Alexa Fluor-647-labelled streptavidin (Molecular Probes).

Chemical synthesis of PIM1 and PIM2

Please see the supporting information for synthetic procedures as well as ^{1}H, ^{13}C and ^{31}P-NMR spectra of new compounds.

Generals in NMR experiments

NMR spectra were recorded with 500, 600, 700 and 800 MHz spectrometers (Bruker BioSpin). The protein solutions in PBS (10 mM sodium phosphate buffer, pH 6.5 or 7.4, 150 mM NaCl) in 99% or 10% (v/v) D_2O were used for NMR experiments. ^{1}H-NMR chemical shifts indicated with parts per million (ppm) were calibrated according to an outer standard chemical shift of 4,4-dimethyl-4-silapentane-1-sulfonic acid (DSS), set at 0 ppm. ^{13}C and ^{15}N chemical shifts (ppm) were calibrated using indirect reference based on the IUPAC-IUB recommended $X/^{1}H$ resonance ratio of 0.251449530 ($^{13}C/^{1}H$) and 0.10132911 ($^{15}N/^{1}H$).[37] NMR data were processed with XWIN-NMR (ver. 3.5) and Topspin (ver. 3.1). The spectra were analyzed with sparky (T. D. Goddard and D. G. Kneller, SPARKY 3, University of California, San Francisco) and displayed using XWIN-PLOT (ver. 3.5).

STD-NMR

1D STD-NMR experiments were performed using a 600 MHz spectrometer with a TXI-probe, and the protein signal at −0.5 or −1 ppm was saturated with 50 ms Gaussian pulse train with 60 times (on-resonance) and reference spectra were obtained with irradiations at 40 ppm (off-resonance). The on-resonance and off-resonance spectra were collected in an interleaved manner, and accumulated into two different data sets. Water suppression was achieved using WATERGATE pulse sequence with a 3-9-19 pulse train. In STD-NMR experiments, 64 scans with 3 repetition loops were required to obtain a good signal to noise ratio, and protein signals were partially suppressed using a 3-10 ms spin lock pulse. In binding epitope analyses, the relative signal intensities were calculated based on the following equation; $\{(I_{off}\text{-}I_{on})/I_{off}\}$ (I_{on}: intensity of on-resonance signals; I_{off}: intensity of off-resonance signals). The values were normalized within each glycan structure using the highest value assigned 100%. Non-labeled ZG16p (50 μM) in PBS (pH 7.4, 99% D_2O) was used for STD-NMR experiments and 100-fold excess of ligands PIM1 **1** and PIM2 **2**, respectively, were titrated into the protein solution.

TR-NOESY

2D ^{1}H-^{1}H NOESY spectra were collected using 700 MHz spectrometer equipped with TCI probe, and probe temperature was set at 10 °C. Residual HDO signal was suppressed using WATERGATE pulse sequence with a 3-9-19 pulse train. NOESY spectra of PIM1 **1** (300 μM) in PBS (500 μL, 99% D_2O, pH 7.4) were collected in the presence of ZG16p (65 μM) or ZG16p-D151N (60 μM). The data was collected in 1024 (F2) × 256 (F1) data points with 32 scans, and the mixing time was set at 150, 250, 350, 500, and 700 ms, respectively. NOESY spectra of PIM2 **2** (300 μM) in PBS buffer (250 μL, 99% D_2O, pH 7.4) was collected in the presence of ZG16p (65 μM) or ZG16p-D151N (60 μM) using micro-cell

(Shigemi). The data was collected in 2048 (F2) × 256 (F1) data points with either 32 or 64 scans, and the mixing time was set at 150, 250, 350, and 500 ms, respectively.

^{1}H-^{15}N HSQC titration experiment

^{1}H-^{15}N HSQC spectra were obtained using a 500 MHz spectrometer equipped with a cryo-TXI probe, and the probe temperature was set at 25 °C. The spectra were collected with 1024 (F2) ×256 (F1) data matrix points with either 4 or 8 scans. To a solution of ^{15}N-ZG16p (0.1 mM) in PBS (pH 6.5, 10% D_2O) added ligands PIM1 **1** and PIM2 **2** (20 mM in PBS with 10% D_2O, pH 6.5), in each molar equivalents, was submitted to ^{1}H-^{15}N HSQC experiments. The weighted average of ^{1}H and ^{15}N chemical shift changes ($\Delta\delta_{avg}$) was calculated using equation; $\Delta\delta_{avg} = [(\Delta\delta_H)^2 + (0.2\times\Delta\delta_N)^2]^{1/2}$, where $\Delta\delta_H$ and $\Delta\delta_N$ are the observed chemical shift changes (ppm) of ^{1}H and ^{15}N, respectively. The backbone amide signals of ^{13}C/^{15}N-ZG16p (0.2 mM) were assigned sequentially via analysis of 3D HNCA, HN(CO)CA, HNCACB, and CBCA(CO)NH spectra obtained using 800 MHz spectrometer equipped with a cryo-TCI probe at 25 °C (Table S1).

Modeling of PIM1-ZG16p complex

The docking of PIM1 to ZG16p was performed using the software package Glide 5.8[31] in Maestro 9.3.5 (Maestro, version 9.3.5, Schrödinger, LLC, New York, NY, 2012.). As a preliminary to docking, the ZG16p (PDB ID; 3APA[5]) was prepared using Protein Preparation Wizard by adding hydrogen, assigning bond orders, optimizing bond lengths, bond angles, and torsion angles. The minimization was performed with the force field OPLS-2005. The ligand glycan was prepared with LigPrep and minimized using the force field OPLS-2005. The receptor glide was generated based on the preexisting glycerol in the initial crystal data. Subsequently, docking study was performed using a standard precision (SP) Glide docking with default parameters. For PIM1, several ligand poses were provided, and the model of highest docking score (−4.0) was the most well agreed to the NMR data. All possible ligand poses were manually evaluated based on the STD-NMR data and the ^{1}H-^{15}N HSQC titration result.

Supplementary Material

Refer to Web version on PubMed Central for supplementary material.

Acknowledgements

This work was supported in part by funding from RIKEN-Max Planck Joint Research Center, the UK Research Council Basic Technology Initiative Glycoarrays (GRS/79268) and Translational Grant (EP/G037604/1), the Wellcome Trust biomedical resource grants WT093378MA and WT099197MA (T.F.), Grant-in-Aid for Young Scientists (B) (No. 24710257) and for Scientific Research (C) (No. 25460054) from the Japan Society for the Promotion of Science (S.H., Y.Y.), and by a SUNBOR GRANT from the Suntory Foundation of Life Sciences (S.H.). We acknowledge BEI Resources (NIAID, NIH) for the Mycobacterial glycoconjugates. We thank members of the Glycosciences Laboratory for their collaboration in the establishment of the neoglycolipid-based microarray system. We thank Dr. Yutaka Muto (RIKEN Yokohama) for his help in acquiring and processing 3D-NMR data. We thank Dr. Yukishige Ito (RIKEN, ERATO) and Prof. Osamu Kanie (ERATO, Tokai University) for enabling us to use the cryoprobe-equipped NMR spectrometer. We thank Dr. Mayumi Kanagawa (RIKEN) for her efforts in trying to co-crystallize ZG16p and PIMs. We acknowledge Mr. Masaki Kato (RIKEN) and RIKEN Integrated Cluster of Clusters (RICC) facility for the trial of MD simulations. We thank Ms. Noriko Tanaka (RIKEN) for secretarial assistance and Dr. Yu-Hsuan Tsai and Dr. Ivan Vilotijevic for valuable discussions regarding the synthesis of PIM1

and 2. We thank Dr. Iria Uhia and Dr. Brian D Robertson (Imperial College London) for specialist opinions on ZG16p-mycobacteria interactions.

References

[1]. Cronshagen U, Voland P, Kern HF. Eur J Cell Biol. 1994; 65:366–377. [PubMed: 7720729]

[2]. Tateno H, Yabe R, Sato T, Shibazaki A, Shikanai T, Gonoi T, Narimatsu H, Hirabayashi J. Glycobiology. 2012; 22:210–220. [PubMed: 21893569]

[3]. Kleene R, Dartsch H, Kern HF. Eur J Cell Biol. 1999; 78:79–90. [PubMed: 10099930]

[4]. Kumazawa-Inoue K, Mimura T, Hosokawa-Tamiya S, Nakano Y, Dohmae N, Kinoshita-Toyoda A, Toyoda H, Kojima-Aikawa K. Glycobiology. 2012; 22:258–266. [PubMed: 21948871]

[5]. Kanagawa M, Satoh T, Ikeda A, Nakano Y, Yagi H, Kato K, Kojima-Aikawa K, Yamaguchi Y. Biochem Biophys Res Commun. 2011; 404:201–205. [PubMed: 21110947]

[6]. Kanagawa M, Liu Y, Hanashima S, Ikeda A, Chai W, Nakano Y, Kojima-Aikawa K, Feizi T, Yamaguchi Y. J Biol Chem. 2014; 286:16954–16965.

[7]. a) Drickamer K. Curr Opin Struct Biol. 1999; 9:585–590. [PubMed: 10508765] b) Figdor CG, van Kooyk Y, Adema GJ. Nat Rev Immunol. 2002; 2:77–84. [PubMed: 11910898] c) Geijtenbeek TB, Gringhuis SI. Nat Rev Immunol. 2009; 9:465–479. [PubMed: 19521399]

[8]. a) Wells CA, Salvage-Jones JA, Li X, Hitchens K, Butcher S, Murray RZ, Beckhouse AG, Lo YL, Manzanero S, Cobbold C, Schroder K, et al. J Immunol. 2008; 180:7404–7413. [PubMed: 18490740] b) Yamasaki S, Matsumoto M, Takeuchi O, Matsuzawa T, Ishikawa E, Sakuma M, Tateno H, Uno J, Hirabayashi J, Mikami Y, Takeda K, et al. Proc Natl Acad Sci U S A. 2009; 106:1897–1902. [PubMed: 19171887] c) Ishikawa E, Ishikawa T, Morita YS, Toyonaga K, Yamada H, Takeuchi O, Kinoshita T, Akira S, Yoshikai Y, Yamasaki S. J Exp Med. 2009; 206:2879–2888. [PubMed: 20008526]

[9]. de Witte L, Nabatov A, Pion M, Fluitsma D, de Jong MA, de Gruijl T, Piguet V, van Kooyk Y, Geijtenbeek TB. Nat Med. 2007; 13:367–371. [PubMed: 17334373]

[10]. a) Tateno H, Ohnishi K, Yabe R, Hayatsu N, Sato T, Takeya M, Narimatsu H, Hirabayashi J. J Biol Chem. 2010; 285:6390–6400. [PubMed: 20026605] b) Feinberg H, Taylor ME, Razi N, McBride R, Knirel YA, Graham SA, Drickamer K, Weis WI. J Mol Biol. 2011; 405:1027–1039. [PubMed: 21112338]

[11]. a) Childs RA, Drickamer K, Kawasaki T, Thiel S, Mizuochi T, Feizi T. Biochem J. 1989; 262:131–138. [PubMed: 2818558] b) Takahashi K, Ezekowitz RA. Clin Infect Dis. 2005; 41:S440–S444. [PubMed: 16237644]

[12]. Laurine E, Manival X, Montgelard C, Bideau C, Berge-Lefranc JL, Erard M, Verdier JM. Biochim Biophys Acta. 2005; 1727:177–187. [PubMed: 15777617]

[13]. a) Cash HL, Whitham CV, Behrendt CL, Hooper LV. Science. 2006; 313:1126–1130. [PubMed: 16931762] b) Lehotzky RE, Partch CL, Mukherjee S, Cash HL, Goldman WE, Gardner KH, Hooper LV. Proc Natl Acad Sci U S A. 2010; 107:7722–7727. [PubMed: 20382864]

[14]. Iovanna J, Frigerio JM, Dusetti N, Ramare F, Raibaud P, Dagorn JC. Pancreas. 1993; 8:597–601. [PubMed: 8302796]

[15]. Ho MR, Lou YC, Wei SY, Luo SC, Lin WC, Lyu PC, Chen C. J Mol Biol. 2010; 402:682–695. [PubMed: 20692269]

[16]. a) Guerin ME, Korduláková J, Alzari PM, Brennan PJ, Jackson M. J Biol Chem. 2010; 285:33577–33583. [PubMed: 20801880] b) Mishra AK, Driessen NN, Appelmelk BJ, Besra GS. FEMS Microbiol Rev. 2011; 35:1126–1157. [PubMed: 21521247]

[17]. a) Feizi T, Fazio F, Chai W, Wong CH. Curr Opin Struct Biol. 2003; 13:637–645. [PubMed: 14568620] b) de Paz JL, Horlacher T, Seeberger PH. Methods Enzymol. 2006; 415:269–292. [PubMed: 17116480] c) Shin I, Park S, Lee MR. Chem Eur J. 2005; 11:2894–2901. [PubMed: 15635679] d) Liu Y, Feizi T, Campanero-Rhodes MA, Childs RA, Zhang Y, Mulloy B, Evans PG, Osborn HM, Otto D, Crocker PR, Chai W. Chem Biol. 2007; 14:847–859. [PubMed: 17656321] e) Liu Y, Childs RA, Palma AS, Campanero-Rhodes MA, Stoll MS, Chai W, Feizi T. Methods Mol Biol. 2012; 808:117–136. [PubMed: 22057521]

[18]. Gilleron M, Quesniaux VF, Puzo G. J Biol Chem. 2003; 278:29880–29889. [PubMed: 12775723]

[19]. Driessen NN, Ummels R, Maaskant JJ, Gurcha SS, Besra GS, Ainge GD, Larsen DS, Painter GF, Vandenbroucke-Grauls CM, Geurtsen J, Appelmelk BJ. Infect Immun. 2009; 77:4538–4547. [PubMed: 19651855]

[20]. Boonyarattanakalin S, Liu X, Michieletti M, Lepenies B, Seeberger PH. J Am Chem Soc. 2008; 130:16791–16799. [PubMed: 19049470]

[21]. a) Patil PS, Hung SC. Chem Eur J. 2009; 15:1091–1094. [PubMed: 19105195] b) Ali A, Wenk MR, Lear MJ. Tetrahedron Lett. 2009; 50:5664–5666.c) Dyer BS, Jones JD, Ainge GD, Denis M, Larsen DS, Painter GF. J Org Chem. 2007; 72:3282–3288. [PubMed: 17385918] d) Ainge GD, Hudson J, Larsen DS, Painter GF, Gill GS, Harper JL. Bioorg Med Chem. 2006; 14:5632–5642. [PubMed: 16697208] e) Stadelmaier A, Schmidt RR. Carbohydr Res. 2003; 338:2557–2569. [PubMed: 14670717] f) Elie CJJ, Dreef CE, Verduyn R, van der Marel GA, van Boom JH. Tetrahedron. 1989; 45:3477–3486.

[22]. Liu X, Stocker BL, Seeberger PH. J Am Chem Soc. 2006; 128:3638–3648. [PubMed: 16536536]

[23]. Ravidà A, Liu X, Kovacs L, Seeberger PH. Org Lett. 2006; 8:1815–1818. [PubMed: 16623558]

[24]. Oltvoort JJ, van Boeckel CAA, Dekoning JH, van Boom JH. Synthesis. 1981:305–308.

[25]. Knerr L, Pannecoucke X, Schmitt G, Luu B. Tetrahedron Lett. 1996; 37:5123–5126.

[26]. a) Mayer M, Meyer B. J Am Chem Soc. 2001; 123:6108–6117. [PubMed: 11414845] b) Mayer M, Meyer B. Angew Chem Int Ed. 1999; 38:1784–1788.c) Meyer B, Peters T. Angew Chem Int Ed Engl. 2003; 42:864–890. [PubMed: 12596167]

[27]. a) Lepre CA, Moore JM, Peng JW. Chem Rev. 2004; 104:3641–3676. [PubMed: 15303832] b) Ardá A, Blasco P, Varon Silva D, Schubert V, André S, Bruix M, Cañada FJ, Gabius HJ, Unverzagt C, Jiménez-Barbero J. J Am Chem Soc. 2013; 135:2667–2675. [PubMed: 23360551]

[28]. Glaudemans CP, Lerner L, Daves GD Jr, Kovac P, Venable R, Bax A. Biochemistry. 1990; 29:10906–10911. [PubMed: 1703008]

[29]. Edison AS, Abildgaard F, Westler WM, Mooberry ES, Markley JL. Methods Enzymol. 1994; 239:3–79. [PubMed: 7830587]

[30]. a) Bourne Y, Zamboni V, Barre A, Peumans WJ, Van Damme EJ, Rouge P. Structure. 1999; 7:1473–1482. [PubMed: 10647178] b) Bourne Y, Roig-Zamboni V, Barre A, Peumans WJ, Astoul CH, Van Damme EJ, Rougé P. J Biol Chem. 2004; 279:527–533. [PubMed: 14561768]

[31]. Friesner RA, Banks JL, Murphy RB, Halgren TA, Klicic JJ, Mainz DT, Repasky MP, Knoll EH, Shelley M, Perry JK, Shaw DE, et al. J Med Chem. 2004; 47:1739–1749. [PubMed: 15027865]

[32]. Zajonc DM, Ainge GD, Painter GF, Severn WB, Wilson IA. J Immunol. 2006; 177:4577–4583. [PubMed: 16982895]

[33]. Schmidt K, Schrader M, Kern HF, Kleene R. J Biol Chem. 2001; 276:14315–14323. [PubMed: 11152672]

[34]. Hase K, Kawano K, Nochi T, Pontes GS, Fukuda S, Ebisawa M, Kadokura K, Tobe T, Fujimura Y, Kawano S, Yabashi A, et al. Nature. 2009; 462:226–230. [PubMed: 19907495]

[35]. a) Satoh T, Chen Y, Hu D, Hanashima S, Yamamoto K, Yamaguchi Y. Mol Cell. 2010; 40:905–916. [PubMed: 21172656] b) Hayashi K, Kojima C. J Biomol NMR. 2010; 48:147–155. [PubMed: 20844927]

[36]. Palma AS, Feizi T, Zhang Y, Stoll MS, Lawson AM, Díaz-Rodríguez E, Campanero-Rhodes MA, Costa J, Gordon S, Brown GD, Chai W. J Biol Chem. 2006; 281:5771–5779. [PubMed: 16371356]

[37]. Wishart DS, Bigam CG, Yao J, Abildgaard F, Dyson HJ, Oldfield E, Markley JL, Sykes BD. J Biomol NMR. 1995; 6:135–140. [PubMed: 8589602]

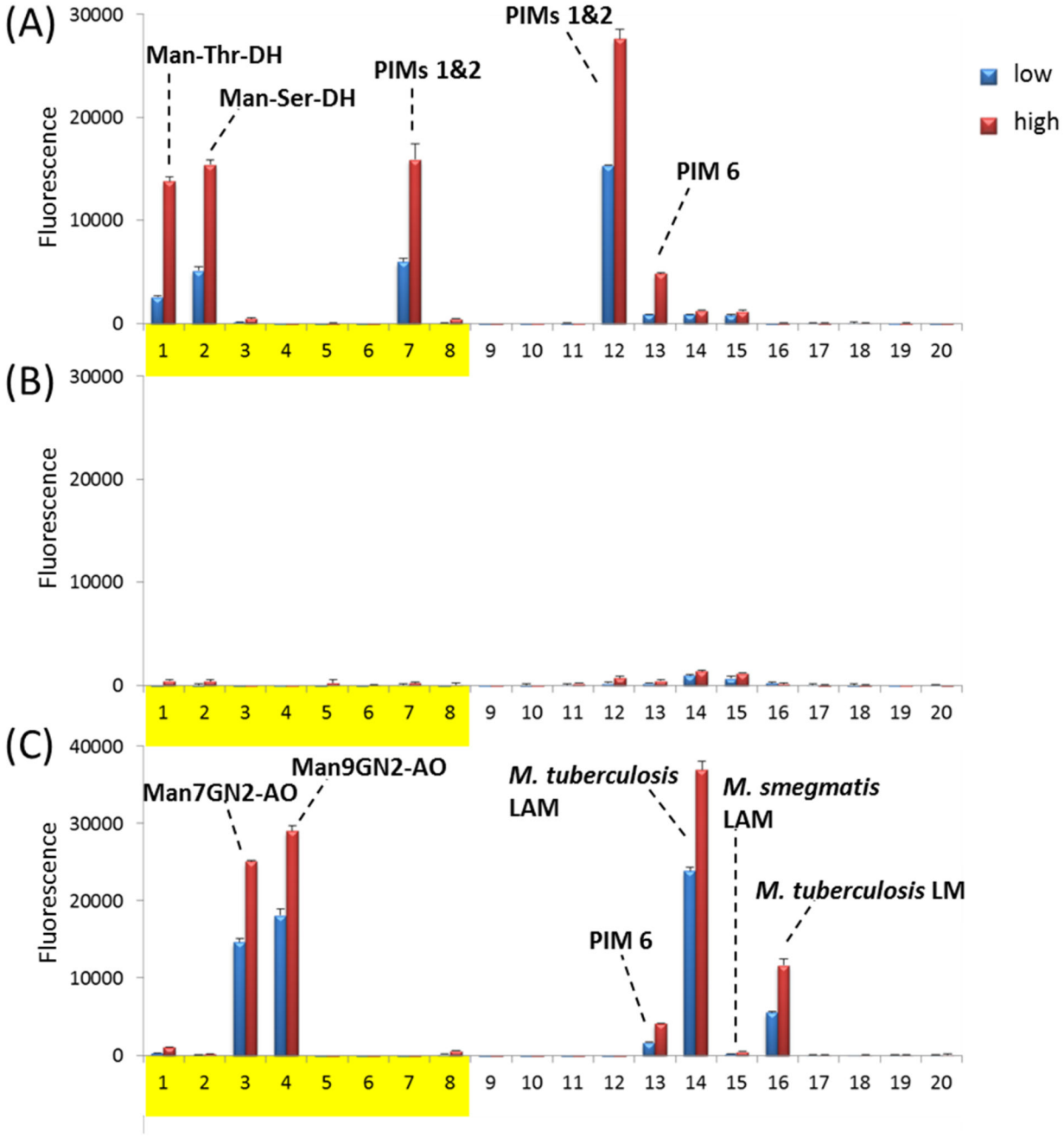

Figure 1.

Microarray analyses using a small pathogen-related array comprising 20 glycan probes (lipid-tagged probes or polysaccharides). The fluorescence intensities for the wild-type ZG16p (A) and D151N mutant (B) are shown. Together, those for the plant lectin Con A (C) was included for comparison. The list of glycan probes and their information are in Table 1. Each probe was printed in duplicate at two levels indicated with a blue bar for low level and a red bar for high level. Shaded in yellow are probes printed at 2 and 5 fmol/spot; the remaining probes were at 0.03 and 0.1 ng/spot.

Europe PMC Funders Author Manuscripts

Europe PMC Funders Author Manuscripts

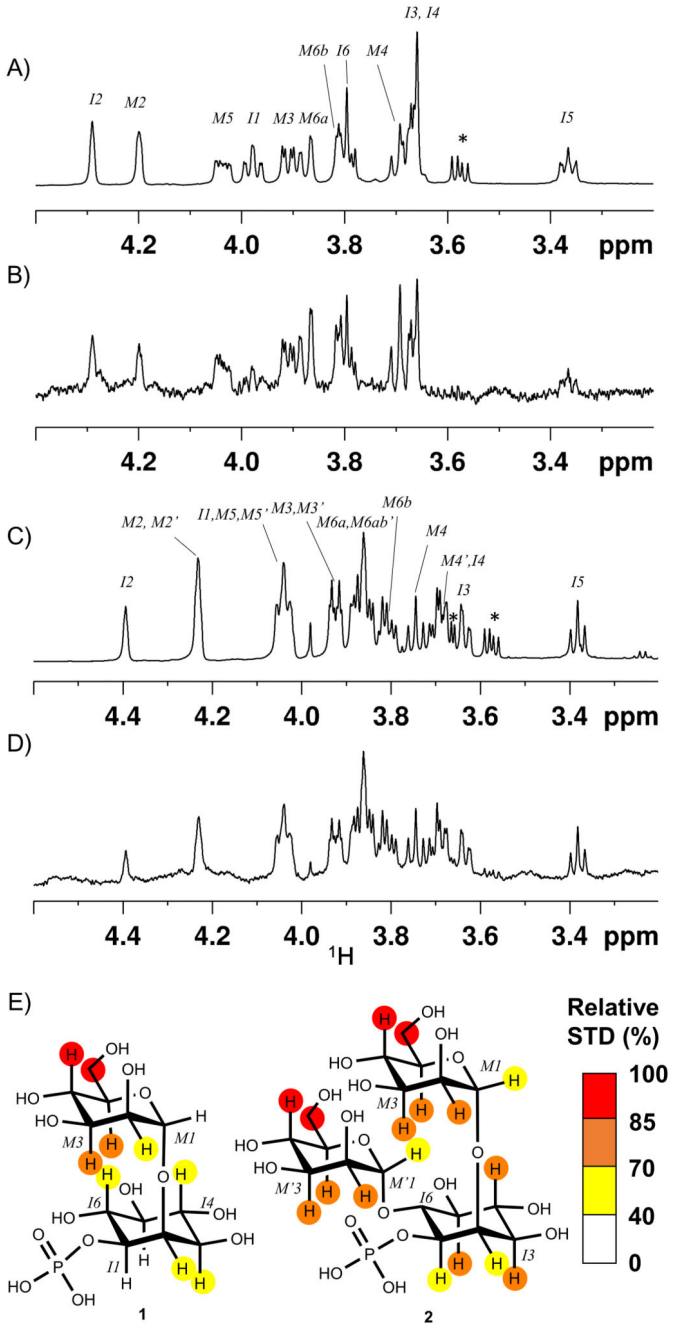

Figure 2.

STD-NMR binding epitope of PIM1 **1** and PIM2 **2** to ZG16p. ^{1}H-NMR off-resonance spectrum (A) and STD-NMR spectrum (B) of PIM1 **1** and ^{1}H-NMR off-resonance spectrum (C) and STD-NMR spectrum (D) of PIM2 **2** in the presence of ZG16p. (E) Binding epitopes of PIM1 **1** and PIM2 **2** were determined by relative STD effects (STD%). In PIM2, STD effects were formally assigned as identical for overlapping signals at M2/M'2, M3/M'3, and M5/M'5. *Signals originating from residual glycerol, included in the buffer used in the

protein purification step. The STD-NMR spectrum was collected at 5 °C using the sample in PBS (pH 7.4) composed with 99% D_2O. *I*; inositol, *M*; mannose

Europe PMC Funders Author Manuscripts

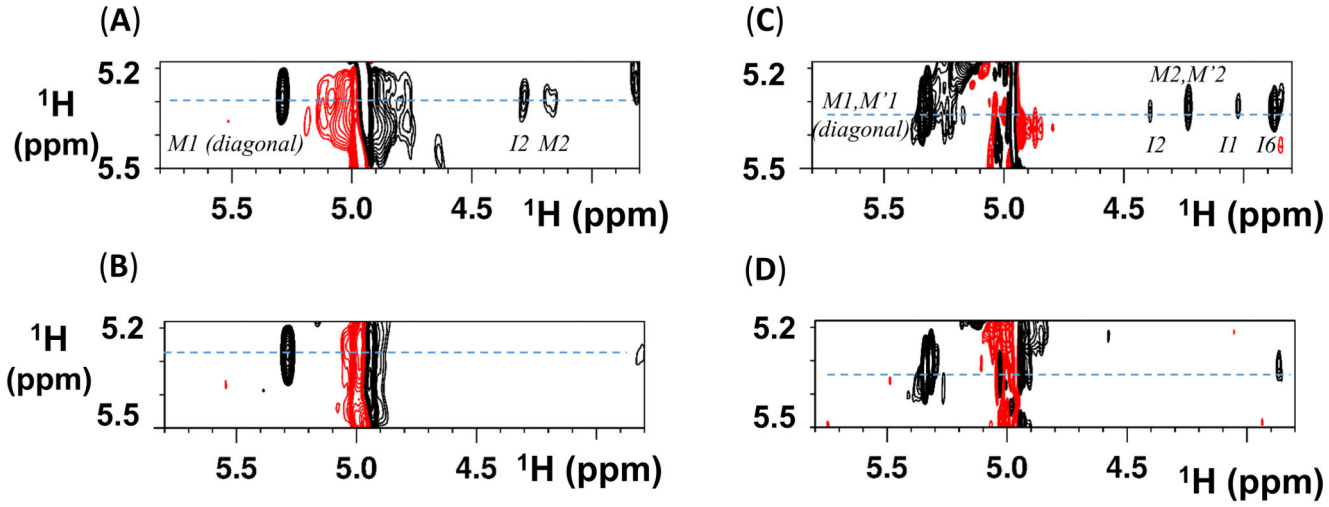

Figure 3.

NOESY spectra of PIM1 and PIM2 in the presence of ZG16p or ZG16p-D151N mutant. NOESY spectra of PIM1 **1** (A) and of PIM2 **2** (C) with ZG16p. Corresponding NOESY spectra of PIM1 **1** (B) and of PIM2 **2** (D) with ZG16p-D151N. The spectra were collected with the mixing time of 250 ms at 10 °C. Red sign is positive and black sign is negative signal. The blue dot lines indicate the chemical shifts of Man-H1 (A and B; PIM1), or Man-H1 and Man'-H1 (C and D; PIM2). Residual HDO signals are observed around 5.0 ppm.

Europe PMC Funders Author Manuscripts

Europe PMC Funders Author Manuscripts

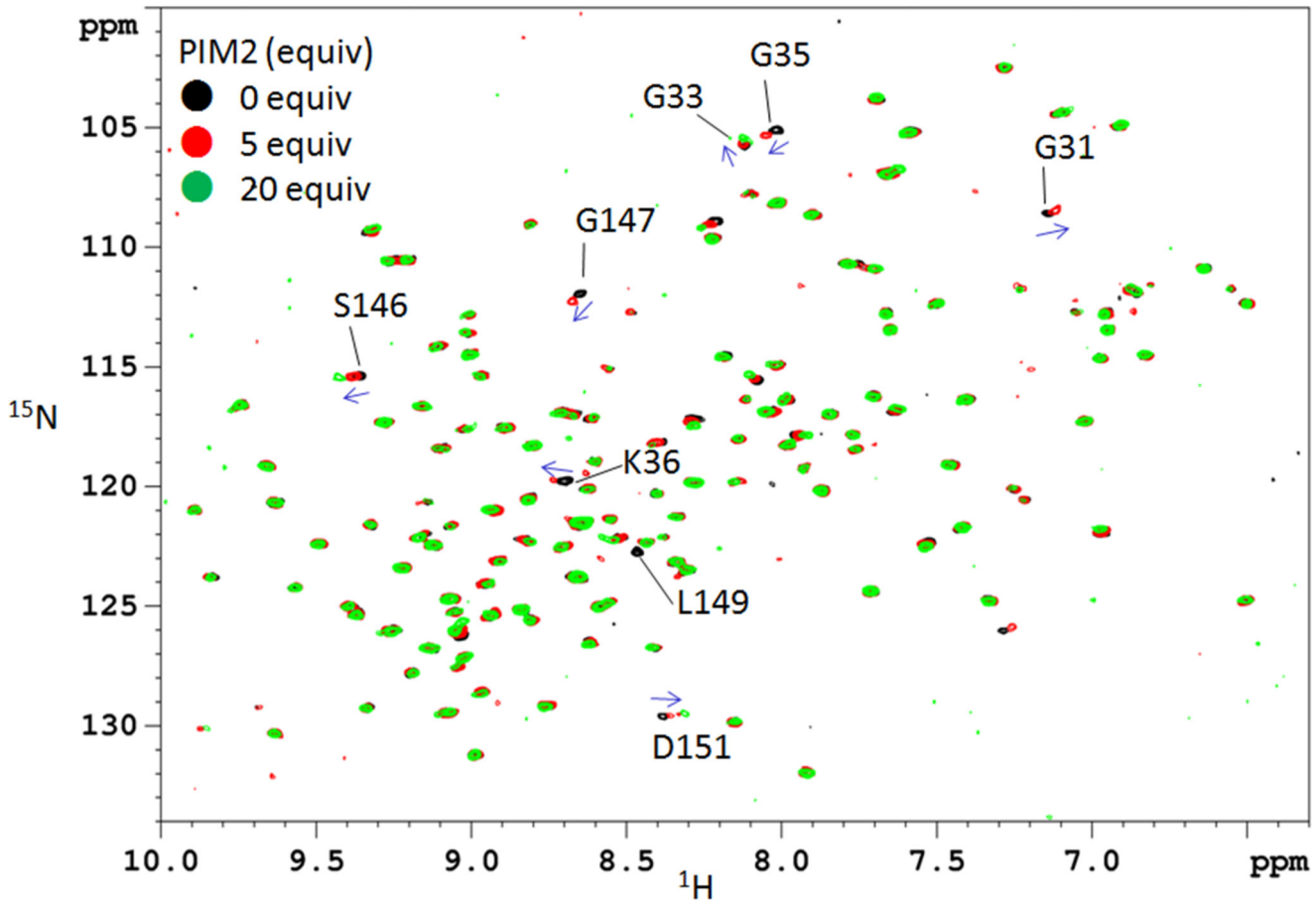

Figure 4.

^{1}H-^{15}N HSQC spectra of uniformly ^{15}N-labeled ZG16p in titration with PIM2 glycan **2**. Black signals are with no ligand, red signals are in the presence of 5 equiv of **2**, and green signals are in the presence of 20 equiv of **2**. Blue arrows indicate direction of the chemical shift changes.

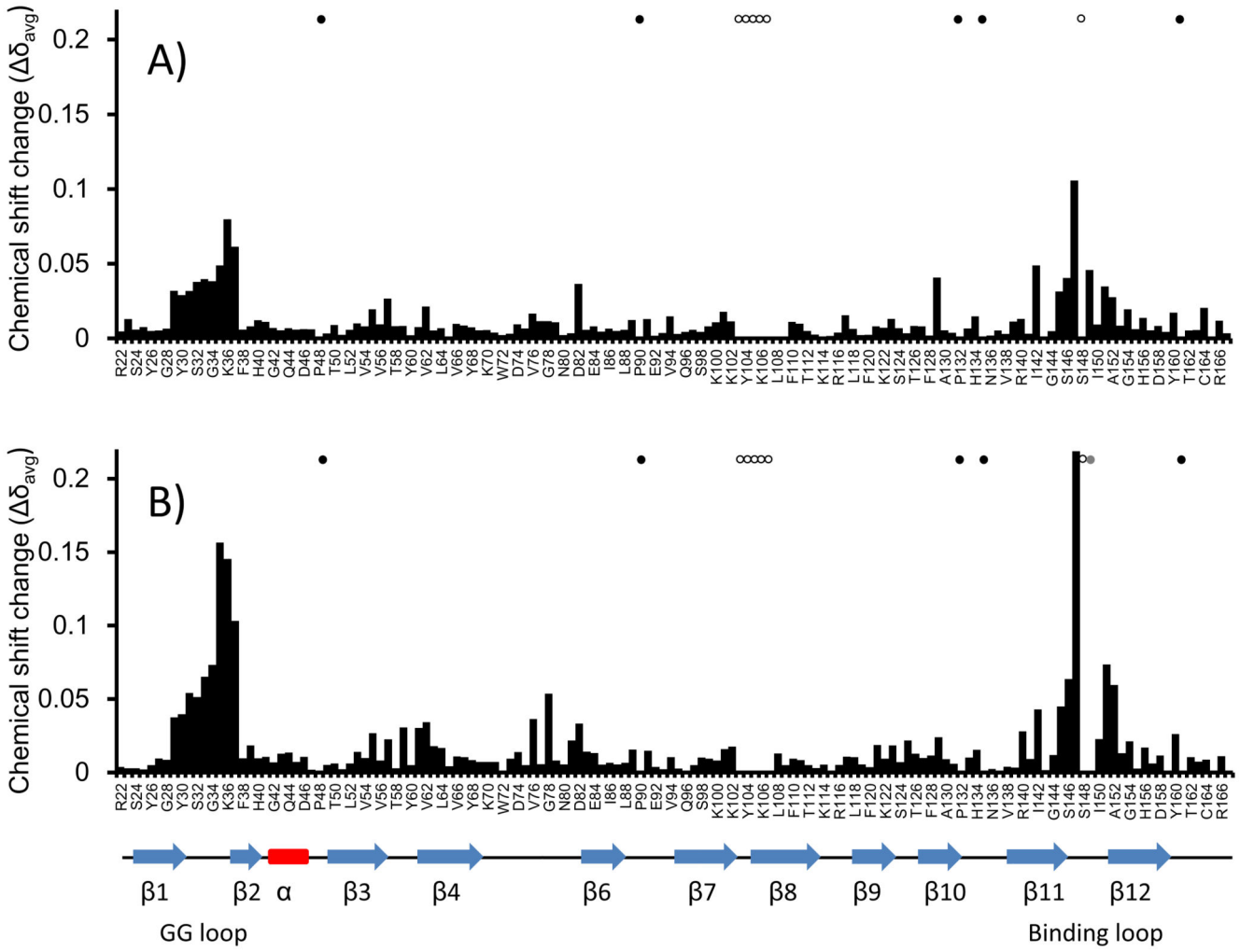

Figure 5.

The weighted $^{1}H/^{15}N$ chemical shift changes ($\Delta\delta_{avg}$) of the backbone amide of ^{15}N-ZG16p upon binding with 20-fold excess PIM1 **1** (A), and 20-fold excess PIM2 **2** (B). Black circles indicate proline, white circles indicate undetermined signals, and gray circles indicate signals that could not be analyzed because of the perturbation effects.

Europe PMC Funders Author Manuscripts

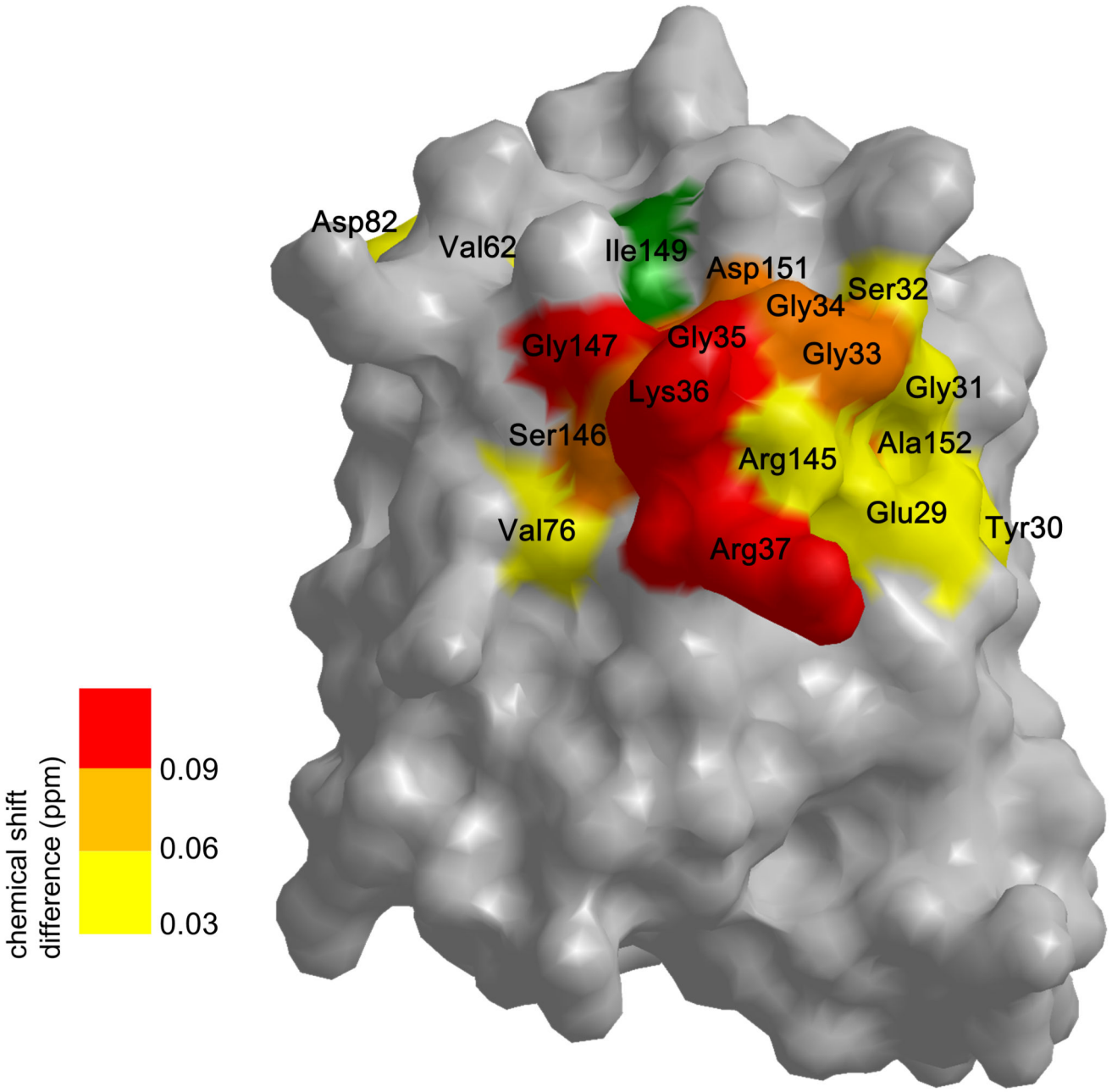

Figure 6.

Mapping the surface residues affected in PIM2-interaction highlighting on the crystal structure of human ZG16p (PDB ID; 3APA).[5] The residues showing $\Delta\delta_{avg}$ within 0.03-0.06 are indicated in yellow, 0.06-0.09 are in orange, and higher than 0.09 are in red. Ile142 shifted in 0.04 ($\Delta\delta_{avg}$) is located inside of the protein. The signal from Ile149 was broadened out upon PIM2 binding and the residue is shown in green.

Europe PMC Funders Author Manuscripts

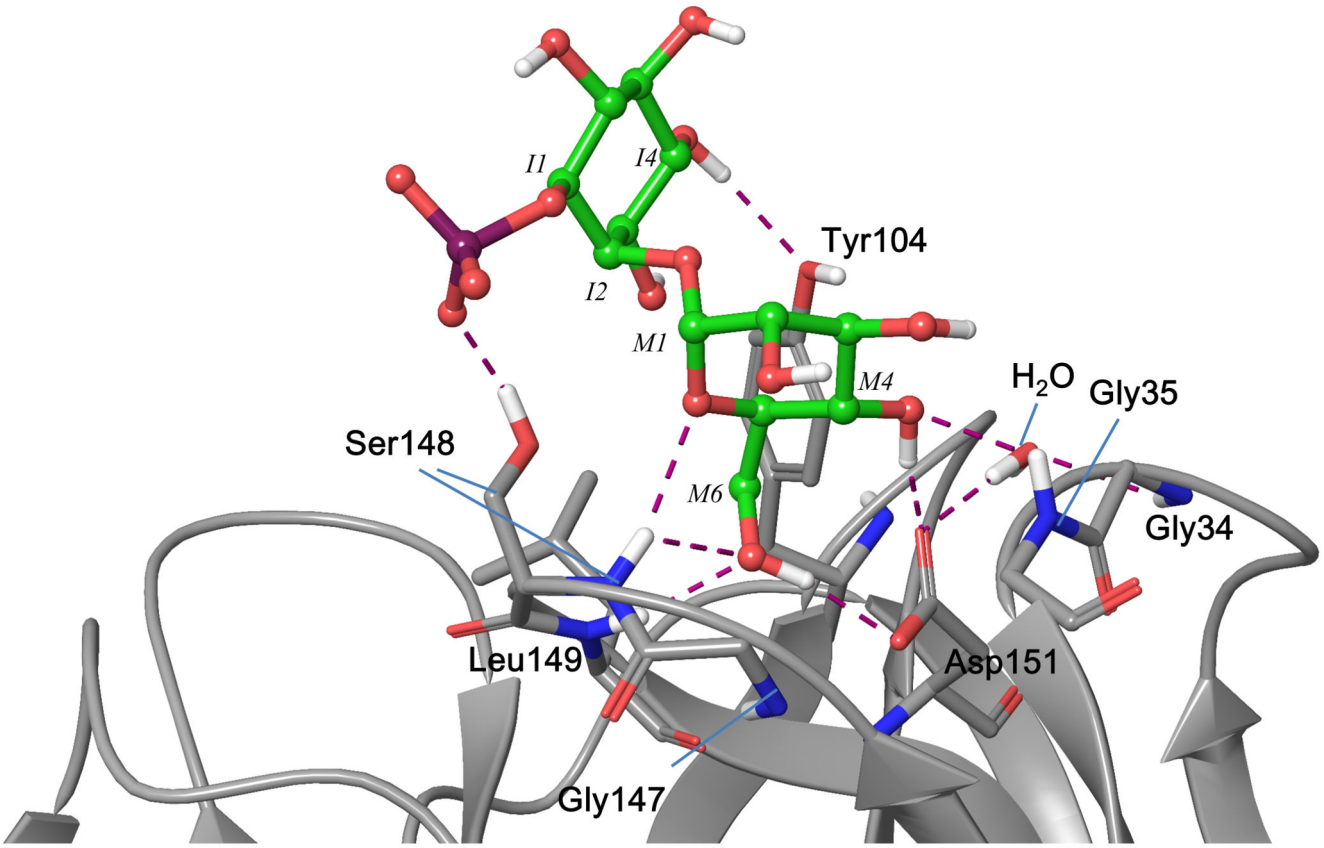

Figure 7.

Binding model of PIM1 glycan to human ZG16p, created with docking simulations. The purple dot lines indicate potential hydrogen bond (3.0 Å).

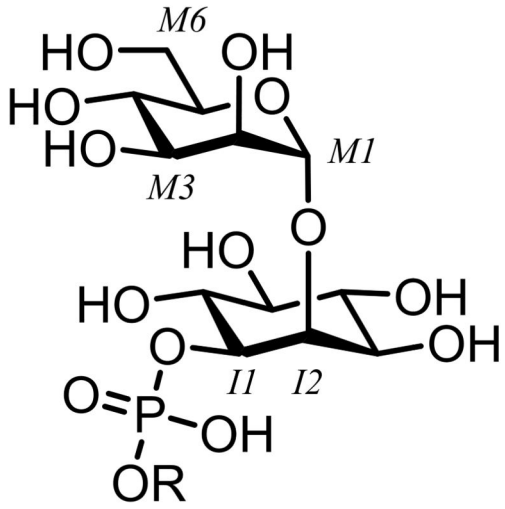

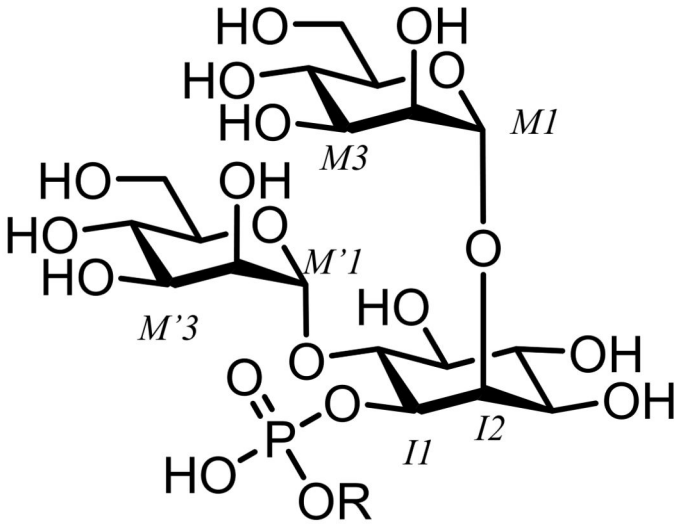

PIM1; R = glycerolipid

1; R = H

PIM2; R = glycerolipid

2; R = H

Scheme 1.
Chemical structures of PIM1 and PIM2.

Europe PMC Funders Author Manuscripts

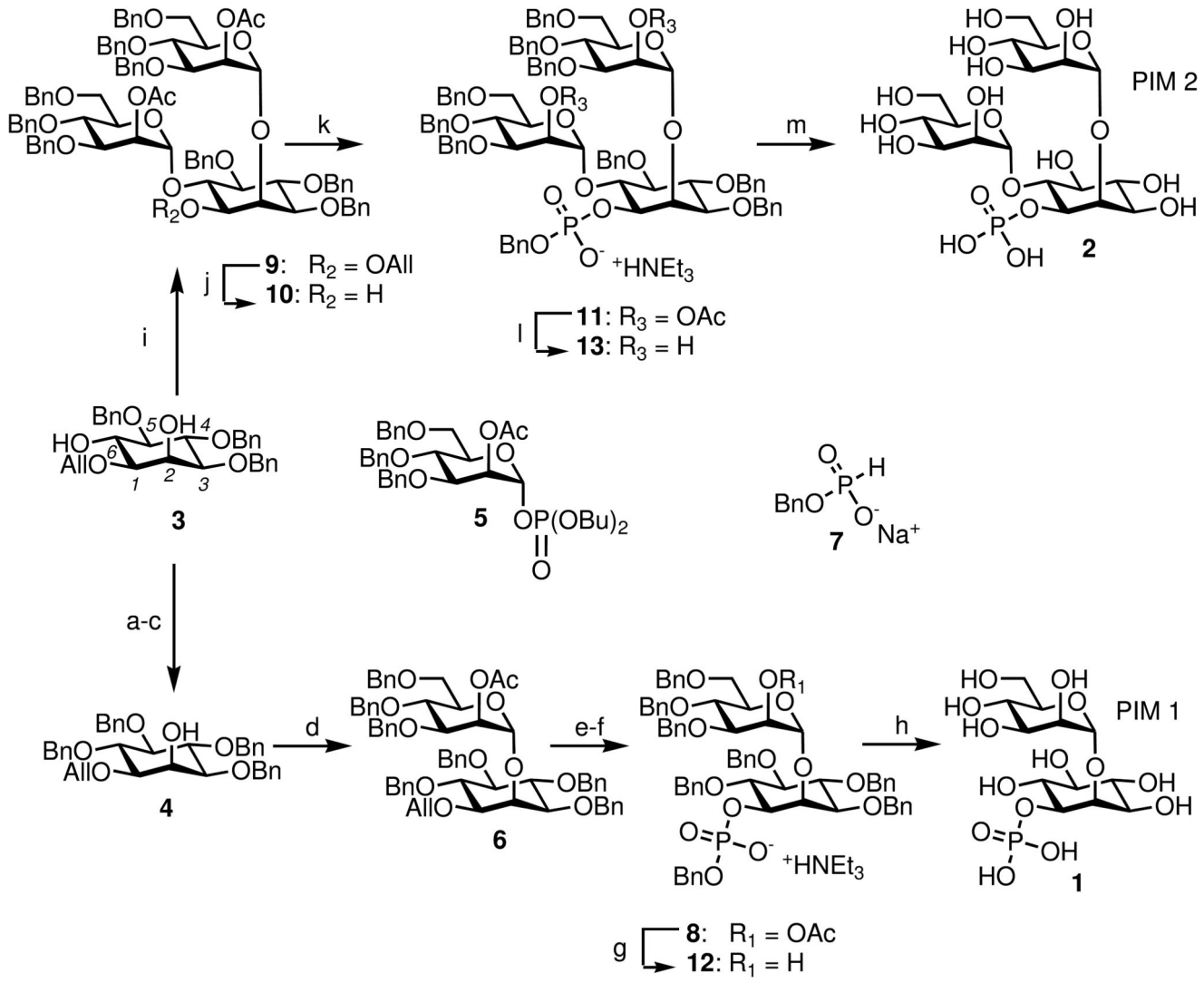

Scheme 2.

Reagents and conditions for synthesis of PIM1 and PIM2 glycans : (a) PMBCl (1 equiv), NaH, DMF, −20 °C, 41% (69% based on recovered starting material); (b) BnBr, NaH, DMF, 0 °C, 90%; (c) $CHCl_3$/TFA (9:1), 93%; (d) **5** (1.3 equiv), TMSOTf, toluene, −40 °C, 84%; (e) i. $[Ir(COD)(PPh_2Me)_2]PF_6$, H_2, THF; ii. $HCl_{(aq)}$, 92%; (f) i. **7**, PivCl, pyridine; ii. I_2, H_2O, 79%; (g) NaH, MeOH, 99%; (h) 10% Pd/C, H_2, MeOH, 98%; (i) **5** (2.6 equiv), TMSOTf, toluene, −40 °C, 62%; (j) $PdCl_2$, CH_2Cl_2/MeOH (1:1), 64%; (k) i. **7**, PivCl, pyridine; ii. I_2, H_2O, 68%; (l) NaH, MeOH, 78%; (m) 10% Pd/C, H_2, MeOH, 92%.

Europe PMC Funders Author Manuscripts

Table 1

List of glycan probes included in microarray analyses.

No.	Probe[a]	Structure
1	Man-Thr-DH	Manα-Thr-DH[b]
2	Man-Ser-DH	Manα-Ser-DH
3	Man7(D1)GN2-AO	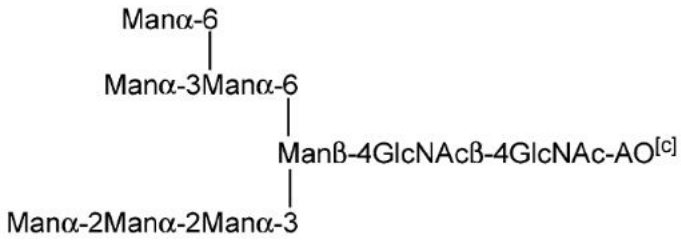
4	Man9GN2-AO	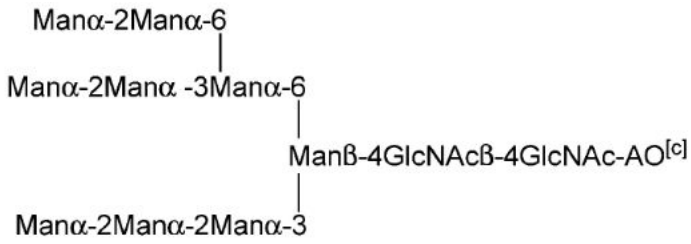
5	*M. tuberculosis* TDM	Purified Trehalose Dimycolate (TDM) from *Mycobacterium tuberculosis*, Strain H37Rv (BEI Number NR-14844)
6	TDB	Trehalose-6,6-dibehenate (TDB), a synthetic analogue of TDM (SIGMA)
7	*M. tuberculosis* PIMs 1&2	Purified PIM 1 & 2 from *Mycobacterium tuberculosis*, Strain H37Rv (BEI Number NR-14846)
8	*M. tuberculosis* PIM 6	Purified PIM 6 from *Mycobacterium tuberculosis*, Strain H37Rv (BEI Number NR-14847)
9	*M. tuberculosis* MME	Purified Mycolic Acid Methyl Esters from *Mycobacterium tuberculosis*, Strain H37Rv (BEI Number NR-14854)
10	*M. tuberculosis* TDM	Purified Trehalose Dimycolate from *Mycobacterium tuberculosis*, Strain H37Rv (BEI Number NR-14844)
11	*M. tuberculosis* Sulfolipid-1	Purified Sulfolipid-1 from *Mycobacterium tuberculosis*, Strain H37Rv (BEI Number NR-14845)
12	*M. tuberculosis* PIMs 1&2	Purified PIM 1 & 2 from *Mycobacterium tuberculosis*, Strain H37Rv (BEI Number NR-14846)
13	*M. tuberculosis* PIM 6	Purified PIM 6 from *Mycobacterium tuberculosis*, Strain H37Rv (BEI Number NR-14847)
14	*M. tuberculosis* LAM	Purified Lipoarabinomannan (LAM) from *Mycobacterium tuberculosis*, Strain H37Rv (BEI Number NR-14848)
15	*M. smegmatis* LAM	Purified LAM from *Mycobacterium smegmatis* (BEI Number NR-14849)
16	*M. tuberculosis* LM	Purified Lipomannan (LM) from *Mycobacterium tuberculosis*, Strain H37Rv (BEI Number NR-14850)
17	*M. tuberculosis* arabinogalactan	Purified arabinogalactan from *Mycobacterium tuberculosis*, Strain H37Rv (BEI Number NR-14852)
18	Pullulan from *Pullularia pullulans*	Mixed-linked α1-4,α1-6 glucose polysaccharide

Europe PMC Funders Author Manuscripts

No.	Probe[a]	Structure
		(Megazyme)
19	Curdlan from *Alcaligenes faecalis*	β1-3 glucose polysaccharide (dissolved in 50 mM NaOH) (Megazyme)
20	Pustulan from *Umbilicaria papullosa*	β1-6 glucose polysaccharide (CalBiochem)

[a]Probes 1-8 were printed at 2 and 5 fmol/spot; the rest were at 0.03 and 0.1 ng/spot. The neoglycolipids (positions 1-4) are from the collection assembled in the course of research in Glycosciences Laboratory.

[b]DH, amino lipid 1,2-dihexadecyl-*sn*-glycero-3-phosphoethanolamine (DHPE)

[c]AO, an aminooxy (AO) functionalized DHPE